Design of a dual-CP gap waveguide fed aperture array antenna

(article starts on next page)

IET Microwaves, Antennas & Propagation

IET The Institution of Engineering and Technology WILEY

ORIGINAL RESEARCH

Design of a dual-CP gap waveguide fed aperture array antenna

Davoud Zarifi[1] | **Ali Farahbakhsh[2]** | **Ashraf Uz Zaman[3]**

[1]School of Electrical and Computer Engineering, University of Kashan, Kashan, Iran

[2]Department of Electrical and Computer Engineering, Graduate University of Advanced Technology, Kerman, Iran

[3]Department of Electrical Engineering, Chalmers University of Technology, Göteborg, Sweden

Correspondence

Davoud Zarifi.
Email: zarifi@kashanu.ac.ir

Abstract

A slot array antenna with dual-circular polarisation (CP) is presented in this paper. To overcome the fabrication and loss challenges in mm-wave frequencies, the gap waveguide technique is utilised. The right and left hand circular polarisation (RHCP and LHCP) radiations are achieved using slots-fed stepped septum polariser on the longitudinal slot arrays. The waveguides and feeding layer are based on ridge gap waveguide. The experimental results demonstrate the $|S_{11}|$ and axial ratio of proposed antenna array are lower than -10 and 2 dB, respectively over the frequency range of 29.1–31.7 GHz. The proposed antenna exhibits the measured peak gain of 27.2 dBic at 30.2 GHz. The results prove that the proposed array antenna is a brilliant choice for 30 GHz-band applications and could be developed to realise larger dual-polarised planar arrays.

KEYWORDS

antenna arrays, millimetre wave antenna arrays, slot antenna arrays

1 | INTRODUCTION

Recently, the mmWaves has drawn considerable attention for high-data-rate wireless communication, automotive radars and wireless gigabit Ethernet. In order to enlarge the propagation distance and to satisfy the specifications mmWave frequencies, various planar antenna arrays have been proposed over the recent years.

Many wireless applications need robust dual polarised antenna which is not sensitive to atmospheric polarisation rotation. Circular polarized (CP) antenna solutions are obvious choice for such applications. Various antennas with different geometries are capable of supporting two orthogonal modes in phase quadrature to create the CP radiation. In this case, a pure CP radiation is indicated by a unitary axial ratio (AR). Generally, two types of feeding can be used in these antennas. The first type is a single-feed at an appropriate location. The other is a dual-feed structure employing an external power divider such as 3-dB hybrid coupler. Up to now, several kinds of CP antennas in the mmWaves have been reported including printed antennas [1–3], planar slot and aperture arrays [4–8]. Achieving a wideband CP performance in the mmWaves bands requires the use of a wideband sequential-rotation feed, a power divider and some phase shifters which leads to the complexity of the design and manufacturing process.

Also, simple, low-cost dual-CP antennas are exceedingly desirable because of their elegant capabilities such as reducing multipath fading, polarisation diversity and frequency reuse. In this case, instead of utilising two separate antennas with right and left hand circular polarisation (RHCP and LHCP) radiations, a single dual-CP antenna with a much smaller size lowers the cost of installation and can also be used to integrate with the other mmWave components.

During the past few years, various dual-CP antennas in mmWave frequencies have been proposed [9–16]. One of the commonly used technologies is substrate Integrated waveguide (SIW). For example, an 8 × 8 element dual-CP cavity backed patch array antenna with SIW feed network is proposed at 60 GHz with a peak gain of 25.8 dBic and 14 dB isolation between the ports [11]. In the design, a six-layer feeding network is utilised to excite the radiating elements, leading to the complexity of the structure. Hollow waveguide antenna arrays are another option, which achieve both CP radiations. For instance, in ref. [14] design of a 16 × 16 element array based on a full-corporate feeding network has been reported with a maximum gain of 32.7 dBic and port-to-port isolation more than 13 dB for Ka-band applications [14]. This antenna has a very complex structure consisting of eight waveguide and radiating layers, which makes the manufacturing and assembly process difficult and expensive. Briefly, at mmWave frequencies,

the main limiting factors affecting the performance of the PCB-based dual-CP antenna arrays are significant dielectric losses, limited power handling and unwanted substrate mode propagation. Also, hollow waveguide-based dual-CP antenna arrays are difficult to be integrated with microwave circuits and need high precision, and high-cost fabrication process which makes them not so suitable for high volume wireless applications.

In this contribution, this paper deals with the design and fabrication of a dual-CP antenna array based on the gap waveguide feeding network. In recent years, the technology of gap waveguide has been employed to design of various antennas and microwave components to remove the fabrication challenges in mmWave frequencies [17–23]. Providing acceptable electrical contact between the structure's various metal layers is a serious challenge in millimetre-wave frequencies. The gap waveguide technology uses the cutoff of a PEC-PMC parallel-plate waveguide to control desired electromagnetic propagation between the two parallel plates without the requirement of electrical contact. In the present work, the proposed subarray is based on double-slot fed square waveguides with septum polariser to achieve both CP radiations for 30 GHz band. Most of CP septum antenna arrays in the literature are single-CP and excited by probes, waveguide flanges or a single slot [24–26]. The main novelty of the work presented in this paper is based on proposing two adjacent centre-fed ridge gap waveguides in order to feed a double-slot fed square waveguide with septum polariser for achieving both RHCP and LHCP radiations in a compact structure. For the very first time, we have introduced the compact septum polarised based square element which can be fed from both ends to realise dual CP performance with a single layer feeding network, which otherwise needs two separate feeing structures for each polarisation. In addition, utilising gap waveguide-based feeding network which remove the challenges of PCB-based and hollow waveguide technologies in mmWave frequencies reinforces the practical aspects of the presented work.

2 | RIDGE GAP WAVEGUIDE

As illustrated in Figure 1, in the ridge gap waveguide structure, two parallel PEC and textured PMC surface are used to create a stop-band and avoid wave propagation [17]. In this structure, by inserting a ridge between the pins, the wave can propagate along the ridge. The apparent advantage of this structure is the possibility of wave propagating between top and bottom metal
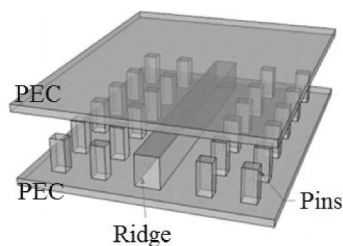
plates without requiring any physical contact between them. Using gap waveguide, only one row is required to prevent energy leakage through the side walls. To obtain the desired stop-band covering 20–40 GHz, the size, height and the periodicity of the pins and air gap chosen in the proposed design is set to be 0.8 mm, 2.4 mm, 2.8 mm and 0.1 mm respectively.

3 | DUAL-CP LINEAR ARRAY ANTENNA

3.1 | Dual-slot fed septum polariser

Configuration of proposed double-slot fed square waveguide with septum polariser is illustrated in Figure 2a. The operation principle of the septum polariser can be explained based on even-odd method [27]. To understand the mode analysis of the structure, a graphical visualisation demonstrated in Figures 2b and c. The excitation at each slot can be decomposed into two even and odd modes and the output of the square waveguide due to slot 1 or slot 2 is simply the summation of its responses to the even and odd modes. As shown in Figure 2b, when slot 1 is excited, the polarisation of propagating electromagnetic wave in the output of square waveguide is LHCP. Similarly, when slot 2 is excited, the polarisation of propagating electromagnetic wave in the output of square waveguide is RHCP, as shown in Figure 2c. If the stepped septum polariser is designed properly, it can be ideally matched and create two
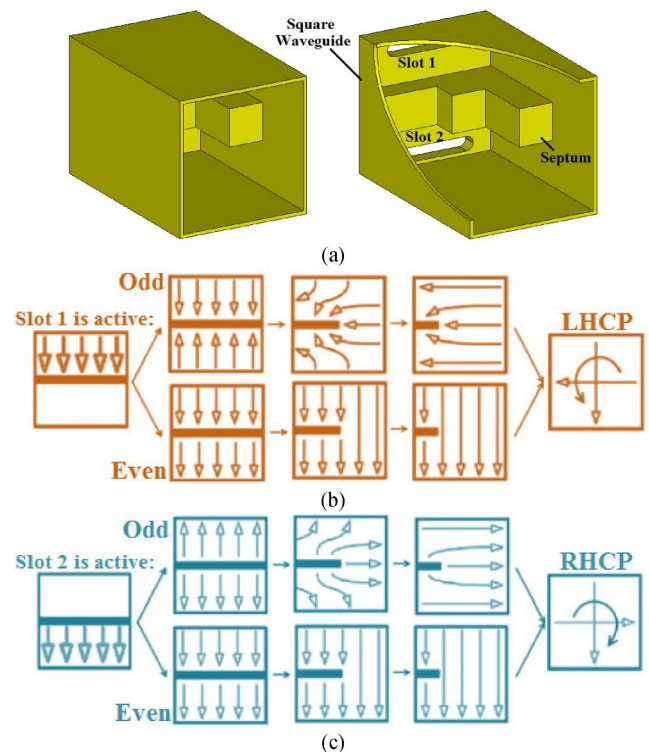

(a)

(b)

(c)

FIGURE 2 (a) Configuration of double-slot fed square waveguide with septum polariser. Propagation of electromagnetic in waveguide when (b) slot 1 is excited, (c) slot 2 is excited.

FIGURE 1 Configuration of ridge gap waveguide.

orthogonal components with the same amplitude and 90º phase difference to achieve CP waves at the output aperture of square waveguide.

3.2 | Dual-CP linear array antenna

In order to achieve a linear array of square waveguide with septum polariser, a feed layer should be designed. Here, series feed technique is used to excite an array of square waveguide with septum polariser, as illustrated in Figure 2a. The proposed configuration includes three main layers as feed layer, waveguides layer, and radiation layer. Observe that in the waveguide layer, two adjacent centre-fed ridge gap waveguides are fed through the coupling slots from the bottom feed network. The coupling slots are made at the centre of the feeding ridges to overcome the challenges such as narrow bandwidth and beam squint. At the beginning and end of each ridge, two steps are made to improve matching and create short circuited sections respectively. At the radiation layer, square waveguides with stepped septum polarisers are employed to transform the polarisation of wave from linear to circular. Ten equi-spaced slots are employed in each ridge gap waveguide to excite the square waveguides. The offset directions are opposite among the adjacent slots to act as quietly similar radiators. By reducing or increasing the number of slots, linear arrays with lower and higher gain can be achieved. Each dual-slot fed cavity with septum polariser can be excited either by a radiating slot in the upper ridge waveguide or by a radiating slot in the lower ridge waveguide. This feature allows RHCP and LHCP to be achieved.

As shown in Figure 3c, when LHCP port is excited, the upper ridge waveguide is active and each cavity with septum polariser is excited by a radiating slot in this waveguide. Due to the positive and negative offsets of the radiating slots, they act as in-phase radiators. As a consequence, a linear array consisting of 10 cavities with septum polarisers with uniform and in-phase excitation is created. As depicted in Figure 3d, a similar situation can be considered for the case where the RHCP port is excited.

The antenna is optimised using the CST Microwave Studio and the final values of the design parameters are listed in Table 1. Figure 4 depicts the $|S_{11}|$ and radiation properties of the antenna column sub-array. The antenna has $|S_{11}| < -10$ dB, AR < 3 dB, peak gain of 18.3 dBic and efficiency higher than 90% from 29 to 31 GHz. The normalised radiation patterns in both principal planes are shown in Figure 5. The electric field distribution of the two adjacent radiating apertures at 30 GHz is shown in Figure 6. It can be observed how the electric field rotates and CP radiation is created.

The dimensions of coupling slot are of crucial importance. In order to investigate the effects of length and width of coupling slot on the input impedance matching of antenna, a parametric study has been performed for these parameters. Figure 7 shows the simulated $|S_{11}|$ of the antenna for these parameters. The results demonstrate that the length and width of coupling slot make strong effects on the performance and frequency bandwidth of the proposed antenna.
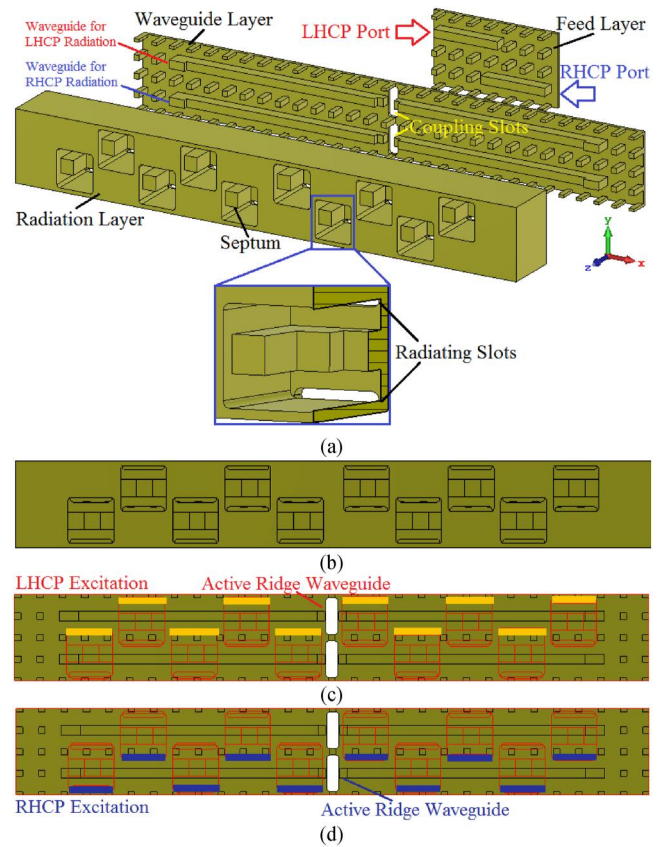

FIGURE 3 (a) Exploded perspective view and (b) top view of the layers of dual-CP linear aperture array antenna. Active waveguide and slots in creating (c) left hand circular polarisation LHCP and (d) right left hand circular polarisation (RHCP) radiation.

TABLE 1 Design parameters of dual-CP linear array antenna.

| Section	Parameter	Value (mm)
Radiating slots	Length	5.16
	Width	0.82
	Offset	1.96
	Spacing	6.42
	Thickness	0.8
Septum polarisers	Waveguide dimensions	5.62 × 5.62
	Septum width	2.12
	Height and width of first step	1.34 × 3.30
	Height and width of second step	0.58 × 0.5
	Height and width of third step	3.50 × 1.18
Coupling slots	Length	4.54
	Width	1.5
	Thickness	0.8
Ridge	Width	1.20
	Height	1.80
	Step near coupling slot	0.98 × 1.10
	Short circuit step	2.40 × 0.60
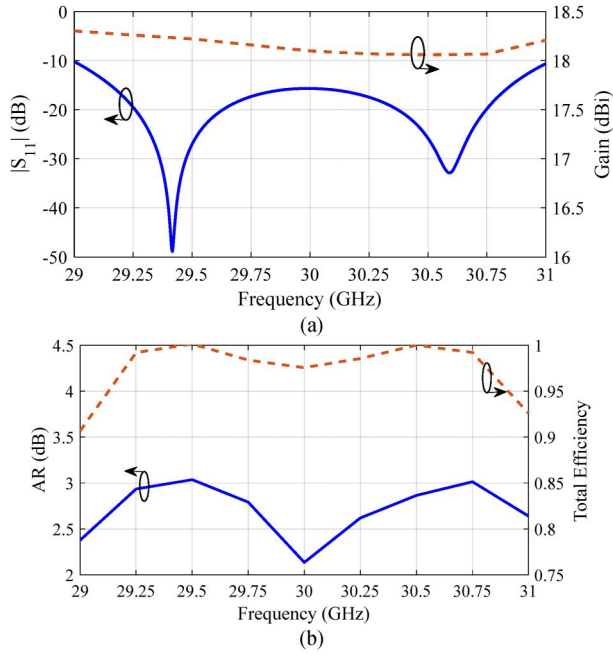
FIGURE 4 Characteristics of dual-CP linear aperture array antenna. (a) $|S_{11}|$ and gain. (b) axial ratio (AR) and total efficiency.
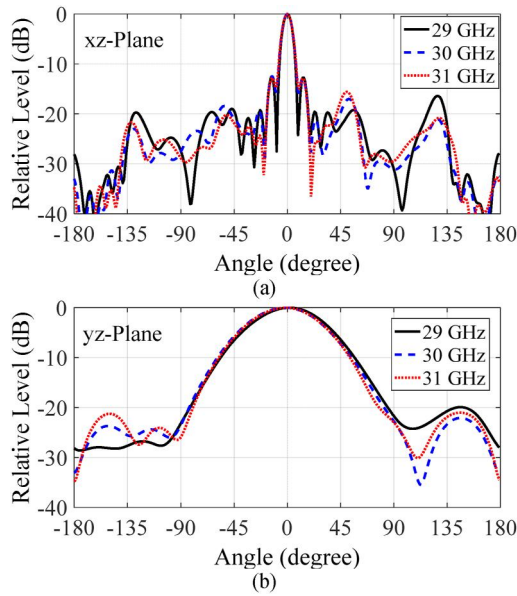

FIGURE 5 Normalised far-field patterns of the dual-CP linear aperture array antenna at frequencies 29, 30, and 31 GHz in both principal planes.

4 | DUAL-CP PLANAR ARRAY ANTENNA

The configurations of two 8-way ridge gap waveguide power dividers for the excitation of dual-CP array antenna are depicted in Figure 8. The left feed network is for exciting the LHCP radiation and the right one is for the excitation of RHCP radiation. As the proposed structure is symmetric, the
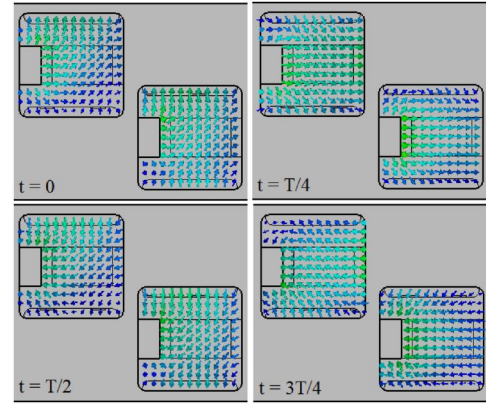

FIGURE 6 Electric field distribution of adjacent radiating apertures at 30 GHz.
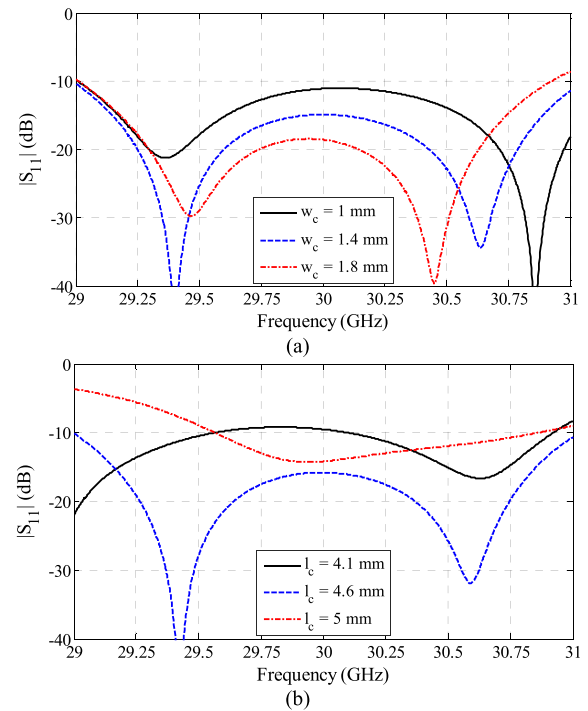

FIGURE 7 Simulated reflection coefficient of dual-CP linear aperture array antenna by changing the coupling slot dimensions.

power divider is in-phase and its output ports have the same phase and equal power division.

To fulfil the matching requirements over the required bandwidth, the V-shaped sections and chamfered corners in the power dividers are optimised. In addition, for feeding the array antenna through a standard Ka-band flange, a simple ridge gap waveguide to WR-28 (7.1 × 3.6 mm²) transition is created. The input matching of the transition is obtained by tuning the extended length of ridge to the waveguide opening. The simulated scattering parameters of the designed 8-way power divider are illustrated in Figure 9. As shown in the figure, the reflection coefficient is less than −20 dB whereas the amplitude imbalance is smaller than ±0.05 dB in the desired frequency range from 29 to 31 GHz.
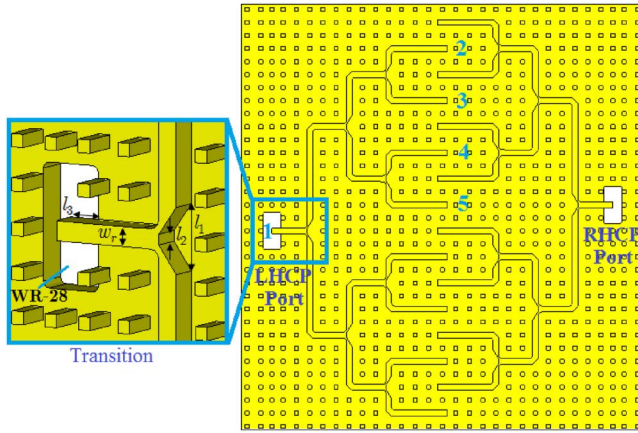
FIGURE 8 The structure of feed network for excitation of left hand circular polarisation (LHCP) and right hand circular polarisation (RHCP) radiations. Top metal plate is not shown in the figure.
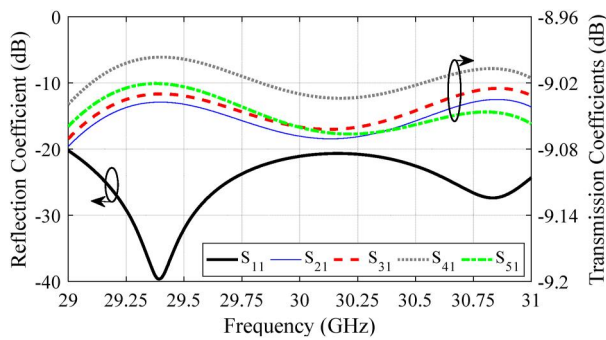

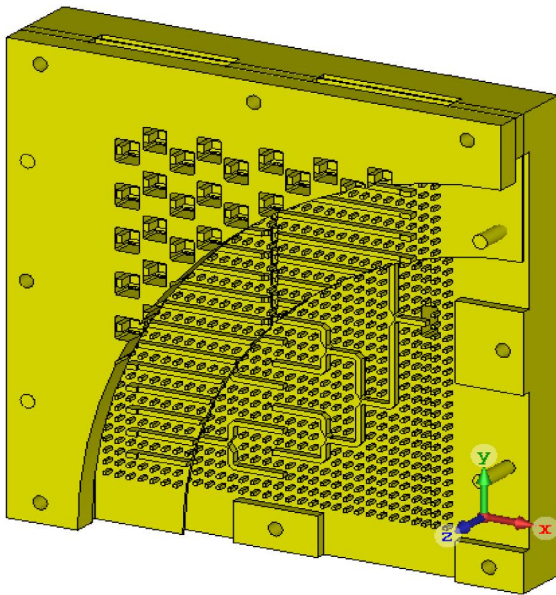**FIGURE 9** Simulated S-parameters of 8-way ridge gap waveguide power divider.

**FIGURE 10** Configuration of dual-CP antenna.

The optimised design parameters of the feed network of planar antenna array are $w_r = 1.2$ mm, $l_1 = 4.68$ mm, $l_2 = 1.19$ mm and $l_3 = 1.92$ mm. The structure of complete dual-CP array antenna is depicted in Figure 10. If there is more than one row of pins between two adjacent rows of the linear array, the radiation pattern of the antenna will have significant grating lobes, which is not desirable. Therefore, the design of the planar array antenna with the smallest possible distance between the adjacent linear arrays has been done. To fulfil the matching and radiation properties over the desired bandwidth, the design parameters of radiation, waveguide and feed layers are optimised. The size of the antenna, counting a few spaces for the screws and alignment pins is $116 \times 116 \times 24$ mm^3.

5 | FABRICATION AND MEASUREMENT

To validate the simulation results, a sample of proposed dual-CP antenna is created using computer numerical control (CNC) milling machine in aluminium material (its electrical conductivity is 3.6×10^7 S/m). The photograph of assembled antenna is illustrated in Figure 11. Eight screws and four alignment pins
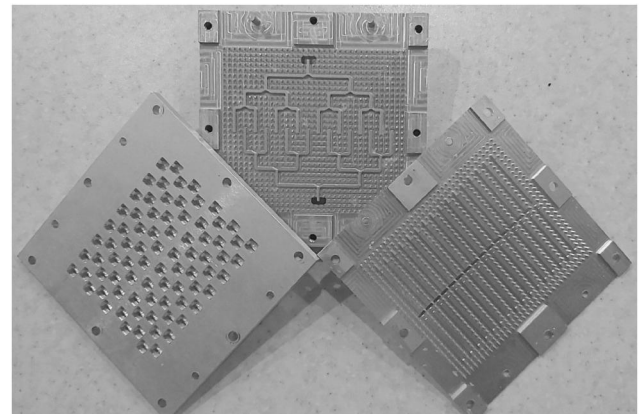
(a)
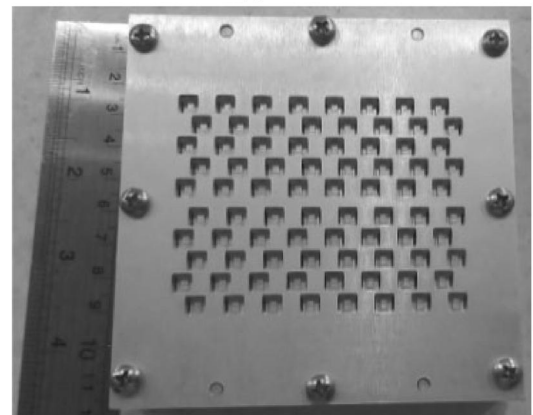
(b)

FIGURE 11 Photographs of unassembled and assembled fabricated antenna.

around the radiation aperture are used to appropriately assemble the antenna.

The input reflection and the two orthogonal port transmission coefficients of the structure are measured by an Agilent network analyser 8722ES. According to the symmetry of planar array antenna, the performance of the antenna is exactly the same with the excitation of each of ports 1 and 2. Therefore, in order to avoid repetition, the simulation and measurement results are presented only for the excitation of port 1. The simulation and measurement results for $|S_{11}|$ and $|S_{21}|$ of antenna are illustrated in Figure 12. The measurement results show the bandwidth of antenna for $|S_{11}| < -10$ dB is 8.6% over 29.1–31.7 GHz, and the LHCP and RHCP ports isolation is better than 14.6 dB at the desired frequency bands. Although the measured impedance bandwidth is less than simulated, the consistency remains satisfactory. As shown in Figure 12b, the gain over 29.4–31.4 GHz is measured to be more than 27 dBic and the radiation efficiency over 80% is obtained for CP radiation. The frequency characteristic of the AR at boresight is also plotted in Figure 12b. The measured AR is less than 2 dB from 29 to 31.9 GHz.

The slight deviations between the results of measurement and simulation could be attributed to misalignments between the different layers, the fabrication tolerance and deviation of Aluminium conductivity, as well as the measurement errors.
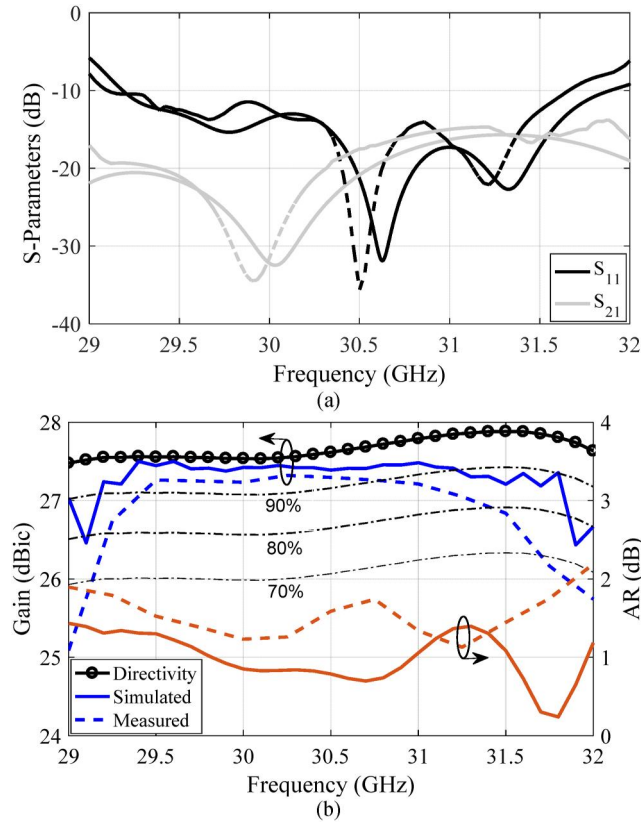
The measurement and simulation results for normalised LHCP radiation patterns of the dual-CP antenna at 30 GHz are shown in Figure 13. The first sidelobe level in both principal values is about −13 dB. In the xz-plane radiation patterns, grating lobes are observed in 55° directions. The presence of grating lobes in xz-plane is predictable due to the distance of more than half-wavelength between the radiation apertures in y-direction. The measured cross polarisations of the antenna are below −26 dB in both principal planes.

The performances of various kinds of reported dual-CP antenna arrays for Ka and higher bands are compared with the present work in Table 2. Most of these antennas have complex multi-layer structures or require special mechanical technologies for fabrication process. Moreover, printed antennas are highly lossy at mmWaves. However, due to use of the gap waveguide technology in waveguide and feeding network layers, the dielectric and ohmic losses of the present work is relatively low. Due to these significant benefits, the presented dual-CP antenna could be a great solution for high frequency applications.

6 | CONCLUSIONS

A simple gap waveguide based dual-CP aperture array antenna topology has been presented and investigated. The array element is a dual-slot fed cavity with septum polariser to achieve both RHCP and LHCP radiations. A CNC milled based prototype of the proposed structure has been manufactured. The measured results indicate the input reflection coefficient is less than −10 dB, the peak gain is more than 27 dBic and AR is smaller than 2 dB in the whole bandwidth from 29.1 to 31.7 GHz. The proposed design could be potentially used in many future mmWaves wireless applications.

FIGURE 12 Simulated and measured results of dual-CP slot array antenna. (a) $|S_{11}|$ and $|S_{21}|$. (b) Gain and axial ratio (AR). The Measurement results are shown with dashed-lines.
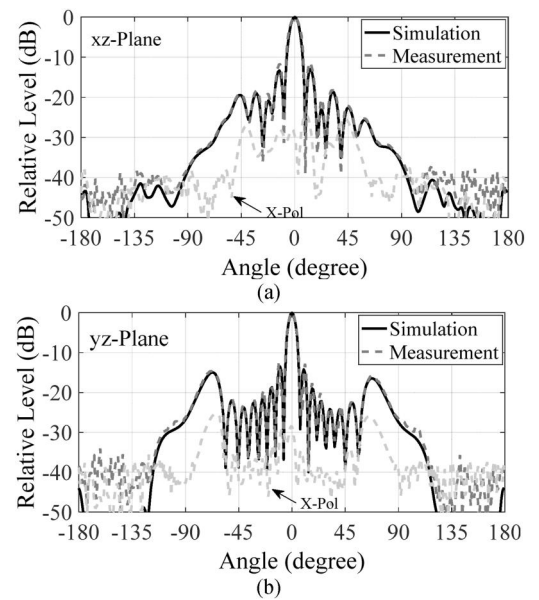

FIGURE 13 Normalised far-field patterns of array antenna at frequency 30 GHz in xz and yz-planes.

TABLE 2 Comparison with some other reported dual-CP array antennas.

Technology	Array size	f_0 (GHz)	B.W (%)	Peak gain (dBic)	Port-to-port isoltaion (dB)	Efficiency (%)	No. of layers
[9]: SIW	15 × 15	94	1.1	26	15	58	2
[10]: SIW	1 × 8	28.15	5	14.2	-	60	4
[11]: SIW	4 × 4	42.2	8.9	19.2	19	-	3
[12]: SIW	8 × 8	61.5	23	25.8	14	59	6
[13]: SIW	8 × 8	60.5	18.2	17.9	17	-	1
[14]: Waveguide	16 × 16	30	16	32.8	13	60	8
[15]: Waveguide	16 × 8	85	2.3	24	20	89	2
[16]: GW	8 × 8	30.25	5	27.5	-	75	4
This work: GW	8 × 10	30.4	8.6	27.2	14.6	80	3

Abbreviations: GW, gap waveguide; SIW, substrate integrated waveguide

AUTHOR CONTRIBUTION

Davoud Zarifi: Conceptualisation; Data curation; Formal analysis; Methodology; Project administration; Resources; Software; Validation; Writing – original draft; Writing – review & editing. **Ali Farahbakhsh**: Conceptualisation; Data curation; Formal analysis; Methodology; Project administration; Resources; Software; Validation; Writing – original draft; Writing – review & editing. **Ashraf Uz Zaman**: Conceptualisation; Methodology; Project administration; Resources; Writing – original draft; Writing – review & editing.

CONFLICT OF INTEREST STATEMENT

The authors certify that they have NO affiliations with or involvement in any organisation or entity with any financial interest (such as honoraria; educational grants; participation in speakers' bureaus; membership, employment, consultancies, stock ownership, or other equity interest; and expert testimony or patent-licencing arrangements), or non-financial interest (such as personal or professional relationships, affiliations, knowledge or beliefs) in the subject matter or materials discussed in this manuscript.

DATA AVAILABILITY STATEMENT

The data that support the findings of this study are available from the corresponding author upon reasonable request.

ORCID

Davoud Zarifi https://orcid.org/0000-0002-0703-6909

REFERENCES

1. Bai, X., Qu, S.-W., Ng, K.B.: Millimeter-wave cavity-backed patch slot dipole for circularly polarized radiation. IEEE Antennas Wireless Propag. Lett. 12, 1355–1358 (2013). https://doi.org/10.1109/lawp.2013.2286196
2. Guntupalli, A.B., Wu, K.: 60-GHz circularly polarized antenna array made in low-cost fabrication process. IEEE Antennas Wireless Propag. Lett. 13, 864–867 (2014). https://doi.org/10.1109/lawp.2014.2320906
3. Zerfaine, A., Djerafi, T.: Ultrabroadband circularly polarized antenna array based on microstrip to SIW junction. IEEE Trans. Antenn. Propag. 70(3), 2346–2351 (2022). https://doi.org/10.1109/tap.2021.3119098
4. Li, M., Luk, K.-M.: A wideband circularly polarized antenna for microwave and millimeter-wave applications. IEEE Trans. Antenn. Propag. 62(4), 1872–1879 (2014). https://doi.org/10.1109/tap.2014.2298246
5. Bisharat, D.J., Liao, S., Xue, Q.: Circularly polarized planar aperture antenna for millimeter-wave applications. IEEE Trans. Antenn. Propag. 63(12), 5316–5324 (2015). https://doi.org/10.1109/tap.2015.2496116
6. Bisharat, D.J., Liao, S., Xue, Q.: High gain and low cost differentially fed circularly polarized planar aperture antenna for broadband millimeter-wave applications. IEEE Trans. Antenn. Propag. 64(1), 33–42 (2016). https://doi.org/10.1109/tap.2015.2499750
7. TomuraSaito, T.Y., Hirokawa, J.: 8 × 2-element 60-GHz-band circularly polarized post-wall waveguide slot array antenna loaded with dipoles. IEEE Trans. Microw. Theor. Tech. 8, 85950–85957 (2020). https://doi.org/10.1109/access.2020.2992922
8. Zhang, M., et al.: A wideband circularly polarized corporate-fed waveguide aperture array in the 60 GHz band. In: IEEE Antennas and Wireless Propagation Letters, vol. 20, pp. 1824–1828 (2021)
9. Cheng, Y.J., Wang, J., Liu, X.L.: 94 GHz substrate integrated waveguide dual-circular-polarization shared-aperture parallel-plate long-slot array antenna with low sidelobe level. EEE Trans. Antenn. Propag. 65(11), 5855–5861 (2017). https://doi.org/10.1109/tap.2017.2754423
10. Park, S.-J., Park, S.-O.: LHCP and RHCP substrate integrated waveguide antenna arrays for millimeter-wave applications. IEEE Antenn. Wireless Propag. Lett. 16, 601–604 (2017). https://doi.org/10.1109/lawp.2016.2594081
11. Xu, J., et al.: A Q-band low-profile dual circularly polarized array antenna incorporating linearly polarized substrate integrated waveguide-fed patch subarrays. In: IEEE Transactions on Antennas and Propagation, vol. 65, pp. 5200–5210 (2017)
12. Zhao, Y., Luk, K.-M.: Dual circular-polarized SIW-fed high-gain scalable antenna array for 60 GHz applications. IEEE Trans. Antenn. Propag. 66(3), 1288–1298 (2018). https://doi.org/10.1109/tap.2018.2797530
13. Zhu, J., et al.: 60 GHz dual-circularly polarized planar aperture antenna and array. IEEE Trans. Antenn. Propag. 66(2), 1014–1019 (2018). https://doi.org/10.1109/tap.2017.2784445
14. Wu, J., et al.: A wideband dual circularly polarized full-corporate waveguide array antenna fed by triple-resonant cavities. IEEE Trans. Antenn. Propag. 65(4), 2135–2139 (2017). https://doi.org/10.1109/tap.2016.2631953
15. Ayoub, F.N., et al.: Cross-slotted waveguide array with dual circularly polarized radiation at W-band. IEEE Trans. Antenn. Propag. 70(1), 268–277 (2022). https://doi.org/10.1109/tap.2021.3090863
16. Ferrando-Rocher, M., et al.: Dual circularly polarized aperture array antenna in gap waveguide for high-efficiency ka-band satellite

communications. IEEE Open J. Antenn. Propagation 1, 283–289 (2020). https://doi.org/10.1109/ojap.2020.3001087

17. Zaman, A.U., Kildal, P.-S.: GAP waveguides. In: Chen, Z.N., et al. (eds.) Handbook of Antenna Technologies. Springer (2016)

18. Ferrando-Rocher, M., et al.: Single-layer circularly-polarized ka-band antenna using gap waveguide technology. IEEE Trans. Antenn. Propag. 66(8), 3837–3845 (2018). https://doi.org/10.1109/tap.2018.2835639

19. Liu, J., et al.: A slot array antenna with single-layered corporate-feed based on ridge gap waveguide in the 60 GHz band. IEEE Trans. Antenn. Propag. 67(3), 1650–1658 (2019). https://doi.org/10.1109/tap.2018.2888730

20. Zhao, Z., Denidni, T.A.: Millimeter-wave printed-RGW hybrid coupler with symmetrical square feed. IEEE Microw. Wireless Compon. Lett. 30(2), 156–159 (2020). https://doi.org/10.1109/lmwc.2019.2960475

21. Farahbakhsh, A.: Ka-band coplanar magic-T based on gap waveguide technology. IEEE Microw. Wireless Compon. Lett. 30(9), 853–856 (2020). https://doi.org/10.1109/lmwc.2020.3009925

22. Farjana, S., et al.: Realizing a 140 GHz gap waveguide–based array antenna by low-cost injection molding and micromachining. J. Infrared Milli Terahz Waves 42(8), 893–914 (2021). https://doi.org/10.1007/s10762-021-00812-8

23. Zarifi, D., Farahbakhsh, A., Zaman, A.U.: Design and development of broadband gap waveguide-based 0-dB couplers for Ka-band applications.

24. Cheng, X., et al.: Analysis and design of a wideband endfire circularly polarized septum antenna. IEEE Trans. Antenn. Propag. 66(11), 5783–5793 (2018). https://doi.org/10.1109/tap.2018.2866584

25. Wang, E., et al.: Wideband high gain circularly polarized antenna array on gap waveguide for 5G applications. In: Proceedings International Symposium on Antennas Propagation (ISAP), pp. 1–3 (2019)

26. Cheng, X., et al.: Compact wideband circularly polarized septum antenna for millimeter-wave applications. IEEE Trans. Antenn. Propag. 68(11), 7584–7588 (2020). https://doi.org/10.1109/tap.2020.2981691

27. Chen, M., Tsandoulas, G.: A wide-band square-waveguide array polarizer. IEEE Trans. Antenn. Propag. 21(3), 389–391 (1973). https://doi.org/10.1109/tap.1973.1140486

IET Microw., Antenn. Propag. 16(11), 718–724 (2022). https://doi.org/10.1049/mia2.12287